Review | Vol. 26, No. 8 | 16 Apr 2018 | OPTICS EXPRESS 9464

Optics EXPRESS

The harmonic state of quantum cascade lasers: origin, control, and prospective applications [Invited]

MARCO PICCARDO,[1,6] PAUL CHEVALIER,[1,6] TOBIAS S. MANSURIPUR,[2] DMITRY KAZAKOV,[1,3] YONGRUI WANG,[4] NOAH A. RUBIN,[1] LAUREN MEADOWCROFT,[1,5] ALEXEY BELYANIN,[4] AND FEDERICO CAPASSO[1,*]

[1]*Harvard John A. Paulson School of Engineering and Applied Sciences, Harvard University, Cambridge, MA 02138, USA*
[2]*Pendar Technologies, 30 Spinelli Place, Cambridge, MA 02138, USA*
[3]*Department of Information Technology and Electrical Engineering, ETH Zurich, 8092 Zurich, Switzerland*
[4]*Department of Physics and Astronomy, Texas A&M University, College Station, TX 77843, USA*
[5]*University of Waterloo, Waterloo, Ontario N2L 3G1, Canada*
[6]*These authors contributed equally to this work.*
[*]*capasso@seas.harvard.edu*

Abstract: The recently discovered ability of the quantum cascade laser to produce a harmonic frequency comb has attracted new interest in these devices for both applications and fundamental laser physics. In this review we present an extensive experimental phenomenology of the harmonic state, including its appearance in mid-infrared and terahertz quantum cascade lasers, studies of its destabilization induced by delayed optical feedback, and the assessment of its frequency comb nature. A theoretical model explaining its origin as due to the mutual interaction of population gratings and population pulsations inside the laser cavity will be described. We explore different approaches to control the spacing of the harmonic state, such as optical injection seeding and variation of the device temperature. Prospective applications of the harmonic state include microwave and terahertz generation, picosecond pulse generation in the mid-infrared, and broadband spectroscopy.

OCIS codes: (140.5965) Semiconductor lasers, quantum cascade; (190.4380) Nonlinear optics, four-wave mixing.

References and links

1. W. W. Chow, S. W. Koch, and M. Sargent, *Semiconductor-Laser Physics* (Springer-Verlag Berlin Heidelberg, 1994), chap. Multimode Operation, pp. 285–328.
2. J. Faist, *Quantum Cascade Lasers* (Oxford University, 2013).
3. H. Choi, L. Diehl, Z.-K. Wu, M. Giovannini, J. Faist, F. Capasso, and T. B. Norris, "Gain Recovery Dynamics and Photon-Driven Transport in Quantum Cascade Lasers," Phys. Rev. Lett. **100**, 167401 (2008).
4. H. Choi, T. B. Norris, T. Gresch, M. Giovannini, J. Faist, L. Diehl, and F. Capasso, "Femtosecond dynamics of resonant tunneling and superlattice relaxation in quantum cascade lasers," Appl. Phys. Lett. **92**, 122114 (2008).
5. C. Y. Wang, L. Diehl, A. Gordon, C. Jirauschek, F. X. Kärtner, A. Belyanin, D. Bour, S. Corzine, G. Höfler, M. Troccoli, J. Faist, and F. Capasso, "Coherent instabilities in a semiconductor laser with fast gain recovery," Phys. Rev. A **75**, 031802 (2007).
6. A. Gordon, C. Y. Wang, L. Diehl, F. X. Kärtner, A. Belyanin, D. Bour, S. Corzine, G. Höfler, H. C. Liu, H. Schneider, T. Maier, M. Troccoli, J. Faist, and F. Capasso, "Multimode regimes in quantum cascade lasers: From coherent instabilities to spatial hole burning," Phys. Rev. A **77**, 053804 (2008).
7. T. S. Mansuripur, C. Vernet, P. Chevalier, G. Aoust, B. Schwarz, F. Xie, C. Caneau, K. Lascola, C.-E. Zah, D. P. Caffey, T. Day, L. J. Missaggia, M. K. Connors, C. A. Wang, A. Belyanin, and F. Capasso, "Single-mode instability in standing-wave lasers: The quantum cascade laser as a self-pumped parametric oscillator," Phys. Rev. A **94**, 63807 (2016).
8. N. Vukovic, J. Radovanovic, V. Milanovic, and D. L. Boiko, "Analytical expression for Risken-Nummedal-Graham-Haken instability threshold in quantum cascade lasers," Opt. Express **24**, 26911–26929 (2016).

#320939 https://doi.org/10.1364/OE.26.009464
Journal © 2018 Received 30 Jan 2018; revised 15 Mar 2018; accepted 16 Mar 2018; published 2 Apr 2018

Optics EXPRESS

9. N. N. Vukovic, J. Radovanovic, V. Milanovic, and D. L. Boiko, "Low-threshold RNGH instabilities in quantum cascade lasers," IEEE J. Sel. Top. Quantum Electron. **23**, 1–16 (2017).
10. H. Risken and K. Nummedal, "Self-Pulsing in Lasers," J. Appl. Phys. **39**, 4662–4672 (1968).
11. R. Graham and H. Haken, "Quantum theory of light propagation in a fluctuating laser-active medium," Zeitschrift für Physik **213**, 420–450 (1968).
12. D. Kazakov, M. Piccardo, P. Chevalier, T. S. Mansuripur, Y. Wang, F. Xie, C. en Zah, K. Lascola, A. Belyanin, and F. Capasso, "Self-starting harmonic frequency comb generation in a quantum cascade laser," Nat. Photonics **11**, 789–792 (2017).
13. J. Faist, F. Capasso, D. L. Sivco, C. Sirtori, A. L. Hutchinson, and A. Y. Cho, "Quantum cascade laser," Science **264**, 553–556 (1994).
14. P. Figueiredo, M. Suttinger, R. Go, E. Tsvid, C. K. N. Patel, and A. Lyakh, "Progress in high-power continuous-wave quantum cascade lasers [Invited]," Appl. Opt. **56**, H15–H23 (2017).
15. T. S. Mansuripur, G. M. de Naurois, W. Metaferia, C. Junesand, S. Lourdudoss, B. Simozrag, M. Carras, and F. Capasso, "Multiple quasi-stable spectral outputs at constant current in a high-power quantum cascade laser," in "International Quantum Cascade Lasers School and Workshop," (Policoro (Italy), 2014).
16. Q. Y. Lu, M. Razeghi, S. Slivken, N. Bandyopadhyay, Y. Bai, W. J. Zhou, M. Chen, D. Heydari, A. Haddadi, R. McClintock, M. Amanti, and C. Sirtori, "High power frequency comb based on mid-infrared quantum cascade laser at $\lambda \sim 9\mu$m," Appl. Phys. Lett. **106**, 51105 (2015).
17. H. Li, P. Laffaille, D. Gacemi, M. Apfel, C. Sirtori, J. Leonardon, G. Santarelli, M. Rösch, G. Scalari, M. Beck, J. Faist, W. Hänsel, R. Holzwarth, and S. Barbieri, "Dynamics of ultra-broadband terahertz quantum cascade lasers for comb operation," Opt. Express **23**, 33270–33294 (2015).
18. R. L. Tober, J. D. Bruno, S. Suchalkin, and G. Belenky, "Zigzag modes in quantum cascade laser emission spectra," J. Opt. Soc. Am. B **31**, 2399–2403 (2014).
19. M. Rösch, I.-C. Benea-Chelmus, C. Bonzon, M. J. Süess, M. Beck, J. Faist, and G. Scalari, "Broadband monolithic extractor for metal-metal waveguide based terahertz quantum cascade laser frequency combs," Appl. Phys. Lett. **111**, 021106 (2017).
20. M. C. Soriano, J. García-Ojalvo, C. R. Mirasso, and I. Fischer, "Complex photonics: Dynamics and applications of delay-coupled semiconductors lasers," Rev. Mod. Phys. **85**, 421–470 (2013).
21. P. Del'Haye, A. Schliesser, and O. Arcizet, "Optical frequency comb generation from a monolithic microresonator," Nature. **450**, 1214–1217 (2007).
22. G. Villares, A. Hugi, S. Blaser, and J. Faist, "Dual-comb spectroscopy based on quantum-cascade-laser frequency combs," Nat. Commun. **5**, 5192 (2014).
23. M. Rösch, G. Scalari, G. Villares, L. Bosco, M. Beck, and J. Faist, "On-chip, self-detected terahertz dual-comb source," Appl. Phys. Lett. **108**, 171104 (2016).
24. J. B. Khurgin, Y. Dikmelik, A. Hugi, and J. Faist, "Coherent frequency combs produced by self frequency modulation in quantum cascade lasers," Appl. Phys. Lett. **104**, 081118 (2014).
25. G. Villares and J. Faist, "Quantum cascade laser combs: effects of modulation and dispersion," Opt. Express **23**, 1651–1669 (2015).
26. G. Villares, S. Riedi, J. Wolf, D. Kazakov, M. J. Süess, P. Jouy, M. Beck, and J. Faist, "Dispersion engineering of quantum cascade laser frequency combs," Optica **3**, 252 (2016).
27. M. Tani, O. Morikawa, S. Matsuura, and M. Hangyo, "Generation of terahertz radiation by photomixing with dual- and multiple-mode lasers," Semicond. Sci. Technol. **20**, S151 (2005).
28. T. Nagatsuma, G. Ducournau, and C. C. Renaud, "Advances in terahertz communications accelerated by photonics," Nat. Photonics **10**, 371–379 (2016).
29. C. Maissen, G. Scalari, F. Valmorra, M. Beck, J. Faist, S. Cibella, R. Leoni, C. Reichl, C. Charpentier, and W. Wegscheider, "Ultrastrong coupling in the near field of complementary split-ring resonators," Phys. Rev. B **90**, 205309 (2014).
30. J. Haas and B. Mizaikoff, "Advances in mid-infrared spectroscopy for chemical analysis," Annu. Rev. Anal. Chem. **9**, 45–68 (2016).
31. I. T. Sorokina and K. L. Vodopyanov, eds., *Solid-State Mid-Infrared Laser Sources* (Springer-Verlag Berlin Heidelberg, 2003).
32. J. R. Freeman, J. Maysonnave, N. Jukam, P. Cavalie, K. Maussang, H. E. Beere, D. A. Ritchie, J. Mangeney, S. S. Dhillon, and J. Tignon, "Direct intensity sampling of a modelocked terahertz quantum cascade laser," Appl. Phys. Lett. **101**, 181115 (2012).
33. S. Barbieri, M. Ravaro, P. Gellie, G. Santarelli, C. Manquest, C. Sirtori, S. P. Khanna, E. H. Linfield, and A. G. Davies, "Coherent sampling of active mode-locked terahertz quantum cascade lasers and frequency synthesis," Nat. Photonics **5**, 306–313 (2011).
34. V.-M. Gkortsas, C. Wang, L. Kuznetsova, L. Diehl, A. Gordon, C. Jirauschek, M. A. Belkin, A. Belyanin, F. Capasso, and F. X. Kärtner, "Dynamics of actively mode-locked quantum cascade lasers," Opt. Express **18**, 13616–13630 (2010).
35. C. Y. Wang, L. Kuznetsova, V. M. Gkortsas, L. Diehl, F. X. Kärtner, M. A. Belkin, A. Belyanin, X. Li, D. Ham, H. Schneider, P. Grant, C. Y. Song, S. Haffouz, Z. R. Wasilewski, H. C. Liu, and F. Capasso, "Mode-locked pulses from mid-infrared quantum cascade lasers," Opt. Express **17**, 12929–12943 (2009).

Optics EXPRESS

36. A. K. Wójcik, P. Malara, R. Blanchard, T. S. Mansuripur, F. Capasso, and A. Belyanin, "Generation of picosecond pulses and frequency combs in actively mode locked external ring cavity quantum cascade lasers," Appl. Phys. Lett. **103**, 231102 (2013).
37. Y. Wang and A. Belyanin, "Active mode-locking of mid-infrared quantum cascade lasers with short gain recovery time," Opt. Express **23**, 4173–4185 (2015).
38. D. G. Revin, M. Hemingway, Y. Wang, J. W. Cockburn, and A. Belyanin, "Active mode locking of quantum cascade lasers in an external ring cavity," Nat. Commun. **7**, 11440 (2016).
39. A. Hugi, G. Villares, S. Blaser, H. C. Liu, and J. Faist, "Mid-infrared frequency comb based on a quantum cascade laser," Nature. **492**, 229–233 (2012).
40. D. L. Boiko, A. V. Antonov, D. I. Kuritsyn, A. N. Yablonskiy, S. M. Sergeev, E. E. Orlova, and V. V. Vaks, "Mid-infrared two photon absorption sensitivity of commercial detectors," Appl. Phys. Lett. **111**, 171102 (2017).
41. M. Piccardo, N. A. Rubin, L. Meadowcroft, P. Chevalier, H. Yuan, J. Kimchi, and F. Capasso, "Mid-infrared two-photon absorption in an extended-wavelength InGaAs photodetector," Appl. Phys. Lett. **112**, 041106 (2018).
42. G. P. Agrawal, *Nonlinear fiber optics* (Academic press, 2007).
43. C. R. Petersen, U. Møller, I. Kubat, B. Zhou, S. Dupont, J. Ramsay, T. Benson, S. Sujecki, N. Abdel-Moneim, Z. Tang *et al.*, "Mid-infrared supercontinuum covering the 1.4–13.3 μm molecular fingerprint region using ultra-high na chalcogenide step-index fibre," Nat. Photonics **8**, 830–834 (2014).
44. C. Xia, M. Kumar, O. P. Kulkarni, M. N. Islam, F. L. Terry Jr, M. J. Freeman, M. Poulain, and G. Mazé, "Mid-infrared supercontinuum generation to 4.5 μm in zblan fluoride fibers by nanosecond diode pumping," Opt. Lett. **31**, 2553–2555 (2006).
45. M. Yu, Y. Okawachi, A. G. Griffith, M. Lipson, and A. L. Gaeta, "Mode-locked mid-infrared frequency combs in a silicon microresonator," Optica. **3**, 854–860 (2016).
46. F. Fuchs, B. Kirn, C. Mann, Q. Yang, W. Bronner, B. Raynor, K. Köhler, and J. Wagner, "Spectral tuning and mode competition of quantum cascade lasers studied by time-resolved Fourier transform spectroscopy," Proc. SPIE **6386**, 63860 (2006).

1. Introduction

Multimode behavior in semiconductor lasers is a complex and intriguing topic [1]. When and why the second mode will start lasing? How do the different modes compete and interact? Such questions are not only fascinating from the perspective of fundamental laser science but also crucial in terms of related applications. A number of mechanisms can affect the gain experienced by the first lasing mode giving origin to multimode operation, including spatial hole burning (SHB), spectral hole burning and population pulsations (PPs). Some of these phenomena, in particular SHB and PPs, play a central role in the operation of quantum cascade lasers [2] (QCLs), unipolar semiconductor lasers characterized by an ultra-fast gain recovery dynamics and strong nonlinear interactions among the optical modes [3, 4], making these lasers an ideal platform for the observation of different multimode regimes.

Coherent instabilities triggering the onset of multimode operation in QCLs have been widely studied in the last decade [5–9]. For instance, it was shown that at a current only fractionally higher than the lasing threshold a coherent instability — reminiscent of the Risken-Nummedal-Graham-Haken (RNGH) instability [10, 11] — occurs in QCLs, where two clusters of modes separated by the Rabi frequency of the primary mode appear [6]. The explanation of this multimode regime has been a matter of debate, but a consensus on its origin now seems to have been reached as due to the combination of both incoherent and coherent contributions to the gain, due to SHB and PPs [7, 9]. More recently, a novel multimode regime in QCLs — the harmonic state — was discovered [7]. This new laser state is characterized by modes separated by several free spectral ranges (FSRs) of the cavity, being fundamentally different from conventional dense multimode states of QCLs, where adjacent cavity modes are populated (Fig. 1). Moreover, the spacing among the modes of the harmonic state was shown to be uniform, by extreme accuracy, proving its nature of optical frequency comb [12]. The ability of the laser to distribute its optical power among few, powerful modes separated by many FSRs (as opposed to many, weaker adjacent cavity modes) has opened previously unforeseen possibilities for QCLs. In this review we will discuss prospects for microwave and terahertz generation, the possibility of mid-infrared pulse generation, and broadband spectroscopy.

Optics EXPRESS

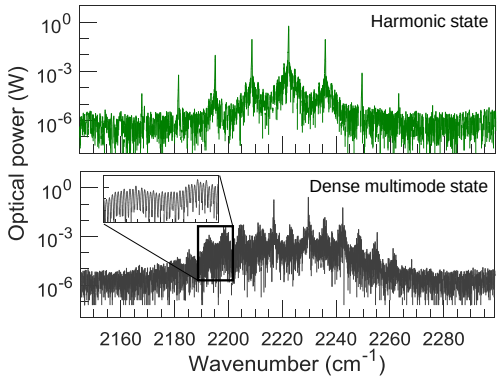

Fig. 1. Harmonic and dense multimode states in QCLs. Optical spectrum of a mid-infrared QCL in the harmonic state with a repetition rate of 400 GHz (top), corresponding to 52 skipped longitudinal modes, much greater larger than that of a QCL operating in a dense multimode regime with a repetition rate of 7.7 GHz (bottom). In both cases, the cavity free spectral range is 7.7 GHz.

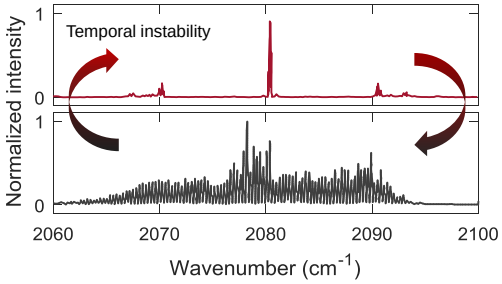

Fig. 2. Spectral instability of a mid-infrared QCL at constant current injection. Every few seconds to a few minutes the laser is observed to hop between a dense multimode state (bottom) and a state characterized by families of modes separated from the central mode by a wide spectral gap (top). The laser is operated at 1.40 J_{th}.

The QCL was invented in 1994 [13], why did it take over 20 years to discover the harmonic state? First of all, its observation required the advent of continuous wave (CW), high-power QCLs, which have become available relatively recently, thanks to the technological development undergone by these devices [14]. Moreover, this state was found to be very sensitive to certain experimental conditions, specifically to delayed optical feedback, whose effects will be discussed in this review, and to the current driving history. Even a poorly aligned collimating lens or a fast current ramp-up in the laser may prevent the occurrence of this state [7]. The first experimental observation that triggered research on the harmonic state was reported by T. S. Mansuripur *et al.* at the International Quantum Cascade Laser School and Workshop in 2014 [15]. It was remarked that a CW high-power QCL would exhibit temporally unstable spectral outputs at constant current injection, repeatedly hopping between a dense multimode state with adjacent cavity modes populated and a state characterized by families of modes separated from the central mode by several FSRs (see Fig. 2). Despite not being a spectrally pure and temporally stable harmonic state, this regime highlighted the possibility of mode skipping in a QCL. Further investigation in different lasers and the proper control of the experimental conditions discussed above led to definite confirmation of the harmonic state, including an extensive report on its experimental phenomenology and its first theoretical explanation [7].

Optics EXPRESS

Here we will review recent findings related to different aspects of this new laser state in QCLs. In Section 2 the origin of the harmonic state will be described. The natural appearance of this regime in the spectral evolution of mid-infrared and terahertz (THz) QCLs will be discussed. A series of studies on the effects of delayed optical feedback on the stability of the harmonic state will be presented, as well as the assessment of its frequency comb nature. A recent theoretical model for its formation will be described. In Section 3 methods to control the spacing of the harmonic state in a given device, such as thermal tuning and optical seeding, will be presented. Finally, in Section 4 future potential applications exploiting the wide spacing exhibited by the harmonic state, such as microwave and THz generation, mid-infrared pulse generation, and broadband spectroscopy, will be discussed.

2. Origin

In this section we present the experimental phenomenology of the harmonic state, followed by a recent theoretical model explaining its formation. Before we begin, we emphasize a few important differences between traveling-wave and standing-wave lasers.

In a traveling-wave laser, once the first mode begins to lase the population inversion is pinned to its threshold value at every position inside the gain medium. While this would seem to prevent the appearance of a second mode, Risken, Nummedal, Graham, and Haken described how multimode oscillation could begin. At the RNGH instability threshold (roughly nine times above the lasing threshold), the lasing mode is strong enough that its interaction with a second frequency provides an additional source of gain — separate from but additive to the background gain provided by the saturated population inversion — that can initiate lasing at that new frequency. This additional source of gain is variously called the coherent gain, parametric gain, or nonlinear gain. Fundamentally, this interaction between the two frequencies is mediated by the material response of the gain medium: the two frequencies beat together, causing a temporal modulation of the intensity of the electric field, which induces a temporal modulation of the population inversion, which then acts back on the two fields and affects their gain. Again, this process is referred to by many names, including the population pulsation, $\chi^{(3)}$-nonlinearity, or four-wave-mixing.

The QCLs under study are standing-wave lasers: two counter-propagating waves form electric field nodes and antinodes, and corresponding regions of high and low population inversion. This spatial modulation of the gain is known as the population grating, or spatial hole burning. Due to this population grating, the gain is not uniformly saturated in a standing-wave laser and as a result, multimode oscillation is perfectly capable of occurring *without* the need for an additional parametric contribution to the gain. In fact, for QCLs this gain is so large that one would expect multimode oscillation to begin when pumped roughly 0.1% above the lasing threshold [7]. Experimentally, however, multimode ocillation begins around 10% above the lasing threshold. In hindsight, this discrepancy begged the question, “Why does the QCL require such a *high* pumping before multimode oscillation begins?".

The discovery of the harmonic state of the QCL answered this question [7]. Whereas in a traveling-wave laser the parametric gain contribution is required to initiate multimode oscillation, in a standing-wave laser the parametric interaction actually reduces the gain seen by the aspiring second mode. This parametric suppression of the gain is strongest for modes adjacent to the primary lasing mode, it becomes weaker as the detuning increases, and eventually turns into a parametric enhancement for widely detuned modes. This explains both why the instability threshold occurs around 1.1 times the threshold pumping (as opposed to 1.001), and why multimode oscillation begins at two sidebands detuned from the primary lasing mode by several FSR, rather than at the adjacent side modes.

Optics EXPRESS

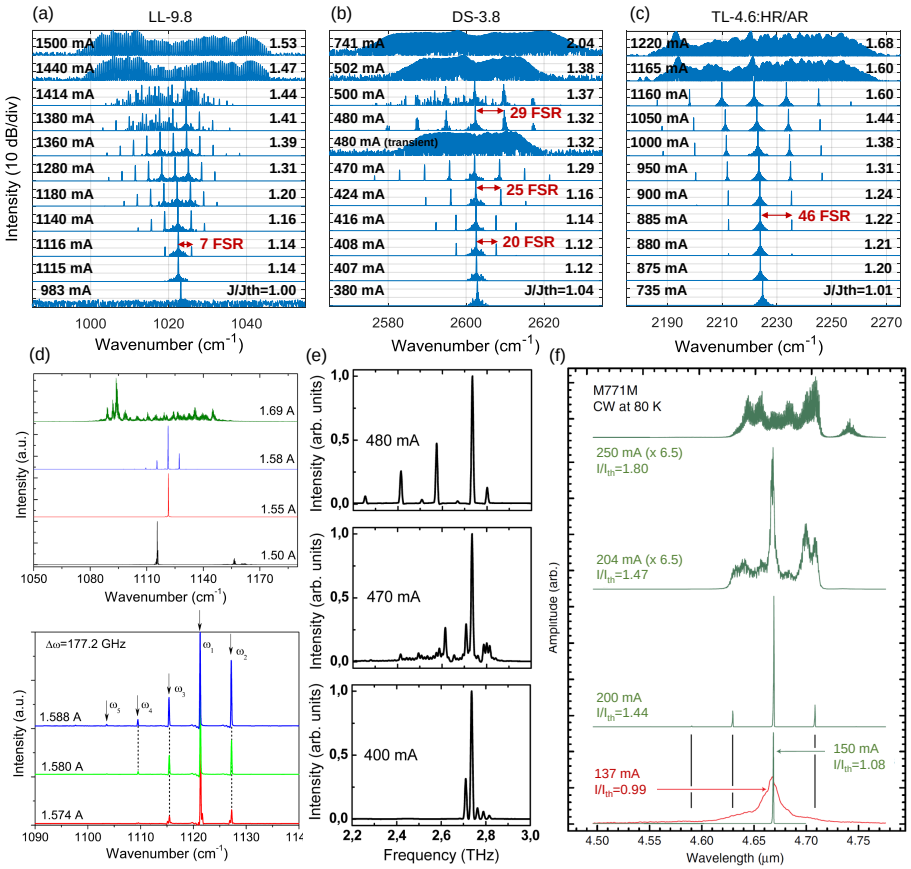

Fig. 3. Spectral evolution of mid-infrared and THz continuous wave QCLs as the current is increased in the laser. (a)-(c) Mid-infrared QCLs emitting at 9.8 μm, 3.8 μm and 4.6 μm. Spectra reproduced from [7]. (d) Mid-infrared QCL emitting at ≈ 9 μm. Both the occurrence of different laser states (top) and the evolution of the harmonic state via four-wave mixing processes (bottom) are shown. Figure reproduced from [16]. (e) Representative emission spectra observed in the evolution of a THz QCL. Figure adapted from [17]. (f) Mid-infrared QCL emitting at 4.7 μm. Figure reproduced from [18].

Optics EXPRESS

2.1. Spectral evolution

The universality of the harmonic state is proven by its observation in completely different QCLs, varying by emission wavelength, bandstructure and device geometry (i.e., characteristics such as device length, waveguide width and facet coatings). The spectral evolution of three CW high-power mid-infrared Fabry-Perot (FP) QCLs emitting at 9.8 μm, 3.8 μm and 4.6 μm, which was reported in [7], is shown in Figs. 3(a)-3(c). These spectra were measured with the QCL being placed about 40 cm from the entrance window of a Fourier transform infrared spectrometer (FTIR) with its output not collimated by a lens, but simply allowed to diverge in order to eliminate the possibility of delayed optical feedback due to reflections from optical elements outside the laser cavity. At a current only fractionally higher (typically 10-20%) than the lasing threshold, the laser evolves from the single-mode regime into the harmonic state, forming symmetric sidebands detuned by several FSRs from the first lasing mode. Increasing the current, more harmonic modes appear preserving a uniform spacing across the whole spectrum. Finally, at high current a transition to the dense state occurs, where adjacent FP modes are populated. Once the current has been increased far into the dense state regime a clean harmonic state cannot be recovered by ramping down the current into the device [7]. The features described here were observed by the authors in several other devices and can be considered as the most general characteristics associated with the appearance of the harmonic state. In some specific cases the spectral evolution of the device may involve more peculiar behaviors, such as a sudden change in the harmonic modes separation or intermittent transitions between the harmonic and dense states at different currents (see, for instance, Fig. 3(b)).

Spectral evolutions of QCLs exhibiting regimes that can be identified as the harmonic state were also reported in [16–18] and are reproduced in Fig. 3(d)-3(f). In [16] in the study of a conventional mid-infrared QCL frequency comb operating at approximately 9 μm Lu *et al.* briefly described the observation of a harmonic state with a spacing of 16 FSR (Fig. 3(d)). Based on the mode proliferation associated with its spectral evolution the authors attributed the origin of this state to a chain of nonlinear four-wave mixing (FWM) processes. Mode skipping was also observed in THz QCLs. In [17] Li *et al.* noticed the generation of harmonic states with a spacing of 2 FSR and 15 FSR from the same device operated at different currents (Fig. 3(e)). A similar behavior was also reported by Rösch *et al.* on THz QCLs using the same active region [19]. We note that in the case of THz QCLs the spectral evolution revealing the appearance of the harmonic states was rather discontinuous (see also Fig. 4(a) in [17]), being quite different from that typically observed in mid-infrared QCLs. In [17] the authors provided a qualitative explanation on the formation of the observed states based on different possible nonlinear mixing processes among the optical modes of the laser. Tober *et al.* observed harmonic states in two CW mid-infrared QCLs emitting around 4.7 μm [18]. Their observation was limited to a narrow range of temperatures around 80 K and a narrow range of currents. (The explanation given in [18] was contradictory as the authors attributed these states to higher order transverse modes but stated that the far-field profile of the laser was single-lobed.)

2.2. Delayed optical feedback effects

In diode lasers, it has been known since the 1960s that delayed self-feedback affects the output spectrum. At first, this feedback was considered a nuisance, because miniscule stray reflections in the optical system that fed back into the laser could increase the relative intensity noise by many orders of magnitude. Motivated by the desire to improve optical communication and optical data storage systems, the topic was thoroughly explored, and delayed feedback became no longer a nuisance, but a tool to study nonlinear dynamics. Delayed feedback is now known to play a role in multimode dynamics, low- and high-dimensional chaos, local and global bifurcations, and stochastic resonance effects, to name a few [20]. We will show that delayed feedback also plays an important role in the spectrum of QCLs. Due to the different time scales involved in QCLs

Optics EXPRESS

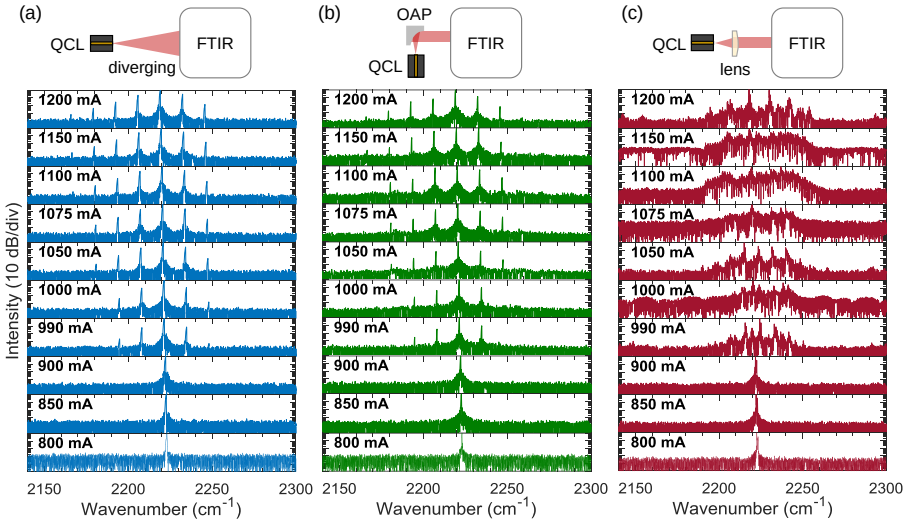

Fig. 4. Spectral evolution of a QCL obtained collecting its spectral output by different schemes. (a) Purely diverging QCL output. (b) QCL output collimated with an off-axis parabolic mirror (OAP). (c) QCL output collimated using a ZnSe lens.

compared to bandgap lasers, QCLs may serve as a test bed for previously inaccessible nonlinear dynamic regimes.

Here we observe that delayed optical feedback can prevent the occurrence of the harmonic state and trigger lasing of adjacent cavity modes. When the laser beam is reflected from some optical components (e.g. a lens) the delay introduces a phase shift and any fluctuations of it will induce a phase noise, translating into frequency shifts. As a result adjacent cavity modes may start lasing, triggering population pulsations in the laser at 1 FSR and resulting in the formation of a dense state.

In order to characterize the effect of delayed optical feedback on the stability of the harmonic state we measured and compared the spectral evolution of a mid-infrared QCL by recording its spectrum by means of different schemes. The studied device is the same as the one reported in [7, 12] (labeled "TL-4.6:HR/AR" and "QCL_1" in the two works, respectively). Few differences in the spectral evolution of the laser with respect to the one presented in [7] (e.g., persistence of the harmonic state rather than the appearance of a dense state around 1200 mA) are attributed to the different value of the temperature set point on the temperature controller (16°C rather than 15°C) and possible changes due to aging of the device. We studied three different experimental configurations, as shown in the schematics of Fig. 4: purely diverging QCL output (the same as in [7]), QCL output collimated with an off-axis parabolic mirror (25.4 mm focal length), or with a ZnSe lens (ISP Optics "ZC-PM-12-12", 13 mm focal length, 0.5 NA). As it can be seen from the measured spectral evolutions, the harmonic state is preserved both in the case of a diverging output and of collimation using an off-axis parabolic mirror. On the other hand, when the output is collimated with the lens the formation of the harmonic state is compromised. This is notable because, as with most semiconductor lasers, high NA collimation optics are desirable given the intrinsic divergence from the laser waveguide. From this perspective these results show that reflective collimators represent the best solution for applications aimed at utilizing the spectral output of the laser operating in the harmonic regime.

To study in a more controlled experiment the effect of feedback on the harmonic state we also carried out an experiment in which the feedback power returning into the waveguide can be varied. The experimental set-up is shown in Fig. 5(a). The output of the QCL is collimated using an

Optics EXPRESS

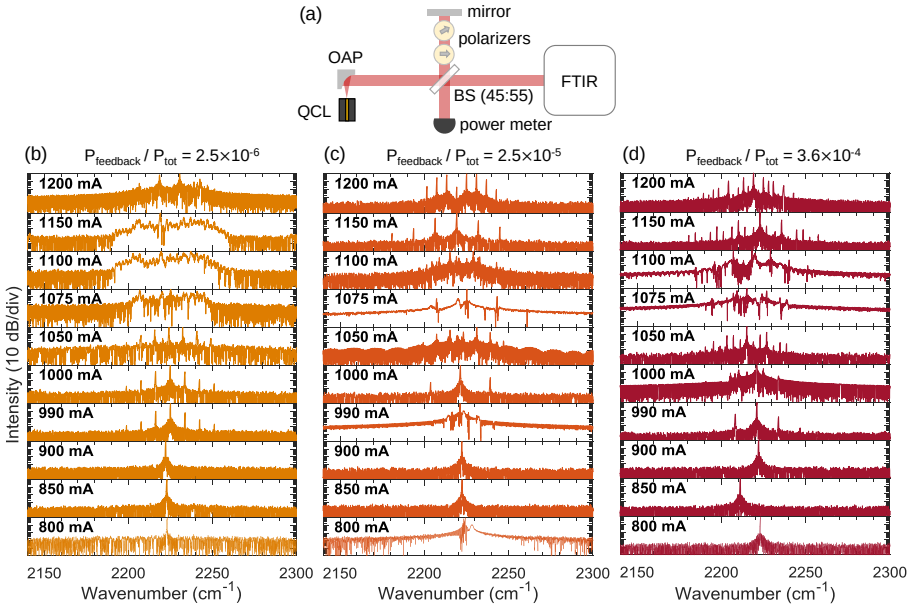

Fig. 5. Effect of delayed optical feedback on the spectral evolution of a QCL. (a) Set-up used for the control of the feedback level. The length of the optical path between the QCL and the mirror is about 30 cm. Mid-infrared polarizers allow for controlled modulation of feedback power. OAP, off-axis parabolic mirror; BS, beam splitter. (b)-(d) Spectral evolutions measured at different levels of feedback power coupled back into the cavity as normalized to the total output power of the QCL.

off-axis parabolic mirror, then separated onto two paths by a beam splitter (splitting ratio 45:55): one sends the beam to the FTIR, the other to a mirror while passing through two mid-infrared polarizers (two are used to allow a higher extinction ratio). The polarizers are used to control the amount of feedback power sent back into the QCL, which can be estimated using a power meter positioned on the remaining arm of the optical set-up (see Fig. 5(a)) and by taking into account the NA of the collimator (≈0.4) and the width of the QCL waveguide (5 μm, note that the QCL emitting facet is AR coated, $R \approx 0.01$). Figures 5(b)-5(d) show the spectral evolution of the QCL upon different levels of feedback power normalized to the total output power of the laser, between 2.5×10^{-6} and 3.6×10^{-4}. As an absolute reference, the total output power of the QCL operating at 1 A is 0.75 W, as measured with a calibrated thermopile (Ophir 3A-QUAD) placed close to the facet. In all cases, even for the smallest level of feedback, the harmonic state is adversely affected, though remnants remain hinting at its presence, while it appears that increasing the feedback level increasingly inhibits the harmonic state. Few anomalous spectra are also observed (e.g., at 1075 mA in Fig. 5(c)), most probably attributable to the QCL hopping between states during acquisition of the FTIR interferogram.

2.3. *Assessment of the frequency comb nature*

Following the first appearance of sidebands at the instability threshold, the spectral evolutions presented in Section 2.1 show that increasing the pumping in the laser generates more sidebands which preserve the initial spacing. This suggests that a CW QCL can self-start into a phase-locked harmonic frequency comb. To assess the comb nature of the harmonic state, in [12] the authors resorted to a multiheterodyne technique [21–23], in which the harmonic spectrum is down-converted from the optical to the microwave domain by means of multiheterodyne

Optics EXPRESS

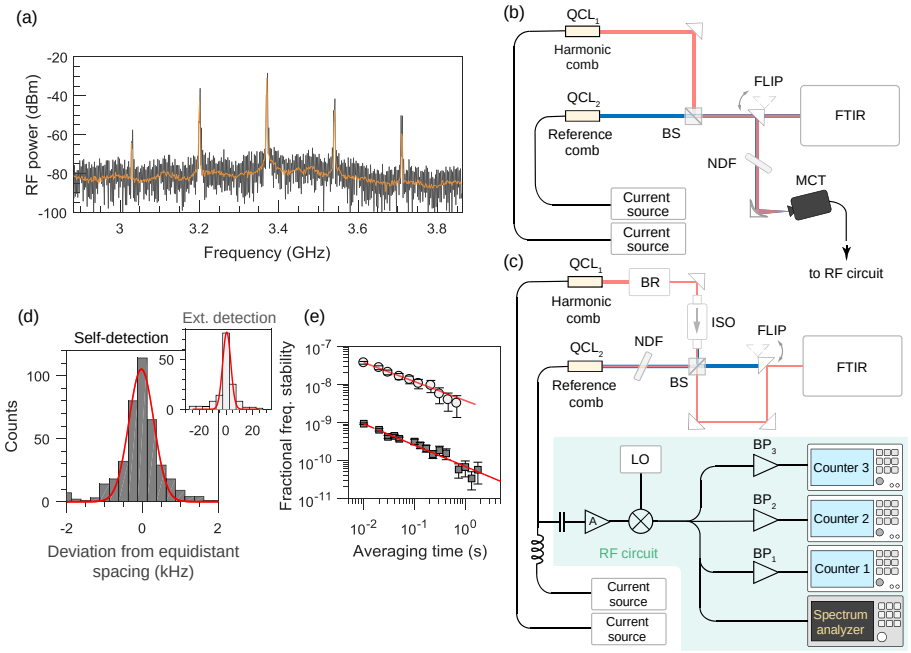

Fig. 6. Assessment of the mode spacing uniformity of the harmonic state. (a) Down-converted harmonic spectrum from the optical to the microwave domain obtained by means of a multiheterodyne technique. The orange trace represents the spectrum averaged over 1000 sweeps of 2 ms. (b),(c) Optical and microwave set-up for the assessment of the comb nature of the harmonic state based on external and self-detection schemes, respectively. BR, beam reducer; ISO, optical isolator; BS, beam splitter; FLIP, flip mirror; NDF, neutral density filter; BP, bandpass filter; LO, local oscillator; A, amplifier; FTIR, Fourier transform infrared spectrometer. (d) Histogram showing the deviation from equidistant spacing of the harmonic state measured with the set-up shown in (c) for a gate time of 10 ms and 402 counts. Inset: histogram obtained with the set-up shown in (b). (e) Fractional frequency stability of the dual-comb system in self-detection mode (squares) versus external detection mode (circles). The self-detected system shows more than an order of magnitude of increase in frequency stability. Figure adapted from [12].

beating with the modes of a finely-spaced reference comb (e.g., Fig. 1, bottom, see [12] for the corresponding narrow beat note). The down-converted spectrum obtained with this method (Fig. 6(a)) forms a microwave comb whose equidistant spacing can be accurately verified using electronic frequency counters. In particular two multiheterodyne schemes were studied: one based on external detection (Fig. 6(b)), where the beating of the optical fields emitted from the two QCLs occurs on an external fast MCT photodetector ensuring the uncoupling of the lasers, and the other based on self-detection (Fig. 6(c)), in which the light emitted from the first laser (QCL_1) is injected, after passing through an optical isolator, into the cavity of the other laser (QCL_2), acting at the same time as a reference comb and a fast photomixer. In both configurations, the beating of the optical fields, whether occurring inside the cavity of the QCL detector or on the fast photodetector, is converted into a microwave signal that is sent to the microwave circuit shown in Fig. 6(c).

To assess the locking of the harmonic modes we further downconvert the multiheterodyne signal with a microwave mixer and select three beatnotes of the spectrum using bandpass filters whose output is fed into three synchronized frequency counters. From the measured frequencies

Optics EXPRESS

a histogram showing the statistics of the deviation from equidistant spacing of the RF comb can be constructed (Fig. 6(d)). The fractional frequency stability of the dual-comb system exhibits an inverse square root dependence on the averaging time indicating the dominance of white-noise frequency modulations in the system giving origin to random and uncorrelated fluctuations following a normal distribution (Fig. 6(e)). This allows to fit the histogram with a Gaussian function. As a result we obtain in the case of self-detection scheme a mean value of $\mu = -27$ Hz and a standard deviation of $\sigma = 329$ Hz, while using the external detection scheme gives $\mu = 0.5$ kHz and $\sigma = 3.0$ kHz. This result verifies the equidistant spacing of the harmonic comb using the self-detection scheme with a relative accuracy of $\sigma/f_c = 5 \times 10^{-12}$, as normalized to the optical carrier frequency of the laser ($f_c = 66.7$ THz), being an order of magnitude smaller than for the measurement based on external detection. This net improvement is due to the higher stability of the multiheterodyne signal in the self-detection scheme. Such improvement in frequency stability can be directly observed by monitoring the multiheterodyne beat spectrum on the spectrum analyzer, as appreciably smaller frequency drifts are seen in self-detection mode.

In addition to the observation of this phenomenon, we advance the hypothesis that the observed improvement in self-detection mode could be due to a locking mechanism occurring inside the injected laser (QCL_2). We exclude a standard master-slave injection locking operation as none of the optical modes of the reference comb can be locked to one of the modes of the injecting laser operating in the harmonic comb regime, otherwise this would lead to a multiheterodyne spectrum with a zero offset, in stark contrast with what we observe (cf. Fig. 6(a), the offset of the RF comb is 142 MHz). However one could imagine the presence of a mechanism locking some of the multiheterodyne beatnotes arising in QCL_2 which would ultimately lead to an increased stability of the multiheterodyne signal in self-detection mode. Consider the following situation: one mode of the harmonic comb injected from QCL_1 into QCL_2 lies close to the middle of two modes of the fundamental comb of QCL_2, spaced by 1 FSR. In this case population pulsations will arise in QCL_2 at two similar frequencies — close to 0.5 FSR — and it may be more favorable for the dynamics of the gain medium of the laser to synchronize these two beatnotes by acting on the carrier envelope offset frequency or on the spacing of the fundamental comb. As a result of this mechanism the frequency noise of the injected laser would correlate with that of the injecting laser, increasing the stability of the multiheterodyne signal. Clearly such process would not be possible in external detection mode as the beating of the optical modes of QCL_1 and QCL_2 takes place in an external photodetector without producing any feedback on the lasers. The proposed mechanism would lead to a multiheterodyne spectrum in self-detection mode with teeth lying in a frequency range close to 0.5 FSR, in agreement with the experimental measurement shown in Fig. 6(a) (0.5 FSR $\approx$ 3.8 GHz in QCL_2). Future studies may investigate in more details the nature of the stability of the multiheterodyne signal in self-detection mode as this configuration presents interesting features that may be exploited in the future in photonic integrated circuits.

In conclusions, these results prove the ability to generate and passively lock harmonic modes in a QCL while skipping adjacent cavity resonances. The demonstrated frequency comb nature of the harmonic state ensures the comb spacing uniformity and holds promise for the generation of microwave or THz tones of high spectral purity based on the beating of its optical modes.

2.4. Theoretical model

In this section we outline the simplest model of nonlinear mode coupling in a laser with a two-level active medium leading to the formation of the harmonic comb spectrum featuring a high degree of parametric suppression of intermediate cavity modes. This model correctly captures the nature of resonant interaction of a multimode field with an active medium. It is not able to make an accurate prediction of laser threshold which would require the microscopic modeling of electron transport, but this is not the focus of this work. For sake of simplicity we consider the case of a high-Q symmetric FP cavity where an orthogonal set of cavity modes can

Optics EXPRESS

be defined. We will calculate the linear parametric gain of the sidebands in the presence of a strong central laser mode, and assume that the actual sidebands in the nonlinear regime will develop at the maximum of the total gain spectrum, obtained from the combined contributions of the Lorentzian and parametric gains. We note the difference of this approach with respect to that of other reported models investigating the impact of FWM on mode-coupling and modal phase relationship in single-FSR-spaced QCL combs, which also rely on Maxwell-Bloch equations but consider an electric field constituted by a large number of optical modes spaced by the cavity roundtrip frequency [24, 25]. The space-time-domain simulations of a harmonic comb formation with a more realistic model for the QCL active region and arbitrary cavity geometry are underway.

We develop a linear theory of the sideband formation due to FWM within a 1D cavity model described by the Maxwell-Bloch equations

$$\begin{aligned}
\partial_t \rho_{ul} &= -\left(i\omega_{ul} + \frac{1}{T_2}\right)\rho_{ul} - i\frac{dE}{\hbar}\Delta, \\
\partial_t \Delta &= -\frac{\Delta - \Delta_p}{T_1} - 2i\frac{dE}{\hbar}(\rho_{ul} - \rho_{ul}^*) + D\frac{\partial^2 \Delta}{\partial z^2}, \\
\partial_z^2 E - \frac{n^2}{c^2}\partial_t^2 E &= \kappa d \partial_t^2 (\rho_{ul} + \rho_{ul}^*),
\end{aligned} \tag{1}$$

where d is the dipole moment of the laser transition, D is the diffusion coefficient of the population inversion Δ, E is the electric field, ρ_{ul} is the off-diagonal density matrix element at the laser transition, n is the effective refractive index of a given transverse waveguide mode, $\kappa = 4\pi\Gamma/c^2 L_p$ with Γ being the optical confinement factor and L_p the length of one period of the active region.

Since both facets have unity reflectivity, the spatial variation of each cavity mode is a standing wave. Specifically, if we assume that the phase of the facet reflection coefficient is zero and the laser cavity is between $z = 0$ and $z = L$, the spatial variation goes like $\cos(kz)$, where $kL = m\pi$ and m is an integer. Taking our cue from the experimental observation, we assume that the lasing field consists of a central mode with frequency ω_0 and two weak sidebands $\omega_\pm = \omega_0 \pm \delta\omega$ with equal and opposite detuning $\delta\omega$, as required by energy conservation in a nonlinear optical process. Also, the wavevector detunings are equal and opposite between the two sidebands corresponding to the phase matching requirement. At the instability threshold the sidebands are weak compared to the central mode, so we can keep only the couplings to the first order of the sideband amplitudes and ignore the creation of fields at other frequencies. We use the set of ansatzes

$$\begin{aligned}
E &= E_0 \cos(k_0 z) e^{-i\omega_0 t} + E_+ \cos(k_+ z) e^{-i\omega_+ t} + E_- \cos(k_- z) e^{-i\omega_- t} + \text{c.c.}, \\
\rho_{ul} &= \eta_0 \cos(k_0 z) e^{-i\omega_0 t} + \eta_+ \cos(k_+ z) e^{-i\omega_+ t} + \eta_- \cos(k_- z) e^{-i\omega_- t}, \\
\Delta &= \Delta_0 + \Delta_2 \cos(2k_0 z) \\
&\quad + \Delta_+ \cos(\delta k z) e^{-i\delta\omega t} + \Delta_- \cos(\delta k z) e^{i\delta\omega t} \\
&\quad + \left[\Delta_{2+} \cos((k_0 + k_+)z) e^{-i\delta\omega t} + \Delta_{2-} \cos((k_0 + k_-)z) e^{i\delta\omega t} + \text{c.c.}\right],
\end{aligned} \tag{2}$$

where $\Delta_- = \Delta_+^*$, $k_0 = n(\omega_0)\omega_0/c$, $\omega_\pm = \omega_0 \pm \delta\omega$ and $k_\pm = k_0 \pm \delta k$. Here we have kept only the relevant terms to the first order. We will first solve for the steady state in the presence of the central mode. Assuming the field of the central mode E_0 to be not too strong so that the Rabi frequency $d|E_0|/\hbar$ is smaller than the saturation value $1/\sqrt{T_1 T_2}$, we can keep terms up to the order $|E_0|^2$. This is equivalent to the $\chi^{(3)}$ approximation for the resonant gain nonlinearity. Proceeding in this way we obtain linear equations for complex sideband amplitudes. The phase

Optics EXPRESS

part of these equations is

$$\left(\frac{n^2(\omega_+)\omega_+^2}{c^2} - k_+^2\right) = -\kappa d\omega_+^2\left(\Re[\alpha_{++}] + \Re[\alpha_{+-}e^{i\phi}]\frac{|E_-|}{|E_+|}\right),$$
$$\left(\frac{n^2(\omega_-)\omega_-^2}{c^2} - k_-^2\right) = -\kappa d\omega_-^2\left(\Re[\alpha_{--}] + \Re[\alpha_{-+}e^{i\phi}]\frac{|E_+|}{|E_-|}\right). \quad (3)$$

The amplitude equations are obtained by taking into account that in the linear theory both sidebands grow in time exponentially with gain g, i.e. as e^{gt}:

$$2\frac{n^2(\omega_+)}{c^2}g = -\kappa d\omega_+\left(\Im[\alpha_{++}] + \Im[\alpha_{+-}e^{i\phi}]\frac{|E_-|}{|E_+|}\right),$$
$$2\frac{n^2(\omega_-)}{c^2}g = -\kappa d\omega_-\left(\Im[\alpha_{--}] + \Im[\alpha_{-+}e^{i\phi}]\frac{|E_+|}{|E_-|}\right). \quad (4)$$

The parameters α are related to the susceptibility tensor as

$$\eta_+ = \alpha_{++}E_+ + \alpha_{+-}E_-^*,$$
$$\eta_- = \alpha_{--}E_- + \alpha_{-+}E_+^*, \quad (5)$$

and the expressions of α are

$$\alpha_{++} = \frac{d}{\hbar}\frac{\Delta_{th}}{\delta\omega + i/T_2}\left[1 + \left(\frac{d|E_0|}{\hbar}\right)^2\left(T_gT_2 + \frac{1}{2}\left(\frac{1}{\delta\omega + i/T_1} + \frac{1}{\delta\omega + i/T_g}\right)\left(\frac{1}{\delta\omega + i/T_2} - iT_2\right)\right)\right],$$
$$\alpha_{+-} = \frac{1}{2}\frac{d}{\hbar}\frac{\Delta_{th}}{\delta\omega + i/T_2}\left(\frac{dE_0}{\hbar}\right)^2\frac{1}{\delta\omega + i/T_1}\left(-iT_2 + \frac{1}{\delta\omega + i/T_2}\right),$$
$$\alpha_{--} = \alpha_{++}|_{\delta\omega\to-\delta\omega},$$
$$\alpha_{-+} = \alpha_{+-}|_{\delta\omega\to-\delta\omega}, \quad (6)$$

where Δ_{th} is the threshold population inversion, and $T_g^{-1} = T_1^{-1} + 4k_0^2D$.

Eqs. (3) and (4) contain 5 unknowns: relative phase $\phi = \arg(E_-^*) - \arg(E_+)$, $\delta\omega$, δk, $|E_-|/|E_+|$ and g. One can solve for any 4 parameters as a function of the fifth. In Fig. 7(a) we plot the gain and phase of the parametric process as a function of $\delta\omega$ at a pumping 10% larger than the lasing threshold. The QCL parameters are those of the laser labeled in [7] as "TL-4.6:HR/AR": emission wavelength $\lambda = 4.5\ \mu$m, gain recovery time $T_1 = 1.7$ ps, dephasing time $T_2 = 74$ fs, dipole moment $d = 1.63$ nm, and sub-threshold GVD $\beta_{GVD} = 400$ fs^2/mm. The material and waveguide GVD are included in the frequency dependence of the refractive index $n(\omega) = 3.23 + 0.5c\,\beta_{GVD}(\omega - \omega_0)$. The gain-related GVD and higher-order dispersive terms are automatically included in the model. In Fig. 7(a) we plot the parametric gain: the maxima of this curve are detuned around 200 GHz from the central mode (26 FSR of a 6 mm long cavity), in qualitative agreement with the experiments [7].

In Fig. 7(b) we plot the phase ϕ as a function of $\delta\omega$. In the vicinity of $\delta\omega = 200$ GHz (i.e. near the gain maxima), ϕ is close to π. This means that the waveform emitted by the QCL is temporally frequency-modulated (FM). This result agrees with the prediction of the theory reported in [7] for the case of symmetric cavities, corresponding to the geometry considered here. It was also predicted in [7] that for lasers with weaker population gratings, which would occur in HR/AR-coated lasers or in lasers with greater carrier diffusion, amplitude-modulated (AM) waveforms (i.e., ϕ closer to zero) could be emitted by QCLs. This prediction will need to be tested in the future, both with more advanced space-time domain simulations of lasers with

Optics EXPRESS

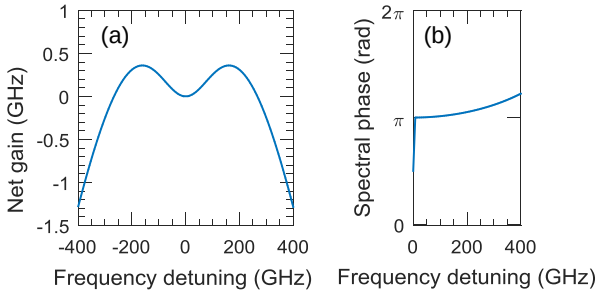

Fig. 7. Theoretical predictions of harmonic comb operation of a QCL. (a) Net gain predicted by the perturbation theory of harmonic comb formation using the device parameters of an existing mid-infrared QCL, at a pump level 1.1 times above threshold. (b) Corresponding spectral phase of the positive sideband, where both the central mode and negative sideband are given amplitudes that are purely real. Figure adapted from [12].

arbitrary cavity geometries, and experiments capable of extracting the relative phases among the modes of the harmonic comb.

While ϕ is close to π for all frequencies of interest, the slow change in ϕ with $\delta\omega$ that is seen in Fig. 7(b) is due to GVD. Recall that we have constrained the two sidebands to have the same frequency detuning. However, in the presence of GVD ω_+ and ω_- would not be modes of the cavity, unless a compensating frequency-pulling effect is provided by the parametric interaction. We can define the pulling exerted by the GVD,

$$\Delta\omega_{pull}\left(\beta_{GVD}\right) = \frac{c\delta\omega^2\beta_{GVD}}{n(\omega_0) + \frac{1}{2}c\omega_0\beta_{GVD}} \tag{7}$$

The compensating pull in the other direction is indeed provided by the parametric interaction, and is given by the right-hand side of Eq. 3. Note that the phase ϕ can adjust to satisfy this equation for various amounts of GVD. However, if the GVD is too large, the nonlinear frequency pulling can not compensate it. We find that a solution to these equations can be found up to the value $\beta_{GVD} \sim 6000$ fs^2/mm. Above this value of GVD no solution exists, indicating that FWM cannot overcome the dispersion and cannot support harmonic comb operation.

As our calculation has shown that gain is larger when ϕ is around π under the assumption $\arg(E_0) = 0$, we may examine the gain spectrum by assuming $\phi \simeq \pi$ and $|E_-|/|E_+| \simeq 1$, then the gain is

$$g \simeq -\frac{\kappa d\omega_0 c^2}{2n^2(\omega_0)}\Im[\alpha_{++} - \alpha_{+-}]. \tag{8}$$

Assuming $\delta\omega \ll 1/T_2$ and $T_2 \ll T_g$, we find that the frequency detuning at the maximum gain is given in the case of the FM instability by

$$\delta\omega^2 = \frac{d|E_0|}{\hbar}\frac{1}{\sqrt{T_2 T_g}} - \frac{1}{T_g^2}. \tag{9}$$

Basically Eq. (9) shows that the spacing of the harmonic state increases with the Rabi frequency and with the inverse of T_2. Moreover it shows that as diffusion becomes stronger (i.e. smaller Tg) the spacing of the harmonic state decreases and eventually vanishes in the limit of weak population grating. We note that the linear theory may predict the value of this spacing only at the onset of the harmonic regime as it assumes a strong central mode and very weak sidebands. In the experiments, as the current is gradually increased above the harmonic state transition, the

Optics EXPRESS

spacing tends to remain constant, as the harmonic sidebands are already seeded with strong fields at particular frequencies, and those frequencies are not going to change with increasing central mode power. However, one laser reported in [7] did exhibit discrete leaps in $\delta\omega$ as the pumping was increased.

The theoretical work and numerical simulations in [8,9] also address the multimode instability in QCLs. The equations that form the basis of the analysis in [8,9] are the same as those presented here, except that they also account for the polarization grating and the diffusion of the polarization. Work is currently ongoing to assess the differences between these two theories. However, in both theories, the instability threshold is predicted to be less than 1.1 times above the threshold for typical QCL parameters.

The harmonic state has also been observed in THz QCLs [17] (see Section 2.1). While the theory discussed above was used to model mid-infrared QCLs in [7, 12], the theory applies generally to standing-wave lasers, but its specific predictions depend of course on the time scales and other parameters of the laser under consideration. In THz QCLs, the population grating is much stronger than in mid-infrared QCLs. This is a direct consequence of the longer wavelength of the population grating. Assuming a similar electron diffusivity in the two types of lasers and a similar upper state lifetime (few ps), an electron in a THz QCL can diffuse over a much shorter distance relative to the grating period, thus preserving the population grating contrast. Even if the THz QCL uses a bound-to-continuum active region design with an upper state lifetime in the tens of ps [17], which allows more time for diffusion, the dominant effect is still the longer wavelength, resulting in a strong population grating. As a result, the incoherent gain contribution to the sidebands is large, which favors sidebands closer to the first lasing mode [7]. However, the competing effect of parametric suppression of nearby sidebands (due to population pulsations) is still sufficient to prevent lasing on modes directly adjacent to the primary mode. Qualitatively, we expect THz QCLs to exhibit harmonic states with a smaller spacing than mid-infrared QCLs. A quantitative comparison between theory and experiment for THz QCLs should be done once more experimental observations are available.

3. Control

The self-starting nature of harmonic combs in QCLs is interesting from the point of view of laser physics and it was shown to be determined by a parametric contribution to the gain of the laser [7, 12], as discussed in the previous section. According to the theory of harmonic comb formation in QCLs, the spacing of the comb is defined by fundamental parameters of the active region, namely the gain recovery time and dephasing time of the laser, in addition to the geometry of the laser cavity (i.e. facet coatings). Applications aimed at exploiting the beating of the harmonic modes, such as those described in Section 4.1, demand a control of the intermodal spacing of these combs. However, fabricating a device with precise values of such parameters for a deterministic design of the spacing of the harmonic comb is a daunting task, which would require bandstructure and dispersion engineering [26]. Therefore it is of paramount importance to find alternative solutions for the control of the spacing of harmonic combs, beyond the fundamental laser design. Here we explore two different approaches, based on thermal tuning and optical seeding of the laser, to shape harmonic frequency combs in QCLs.

3.1. Thermal tuning

We carried out a cryogenic experiment by inserting one of the mid-infrared QCLs studied in [7] (labeled "DS-3.8" therein) into a continuous flow cryostat (Janis ST-100) cooled with liquid nitrogen, for which the temperature was stabilized with a integrated heater and a temperature controller. The spectral output of the QCL at temperatures ranging between approximately 80 and 280 K is measured using an FTIR. The harmonic state is observed across the entire range of studied temperatures. At each temperature, the current was ramped up from below threshold until

Optics EXPRESS

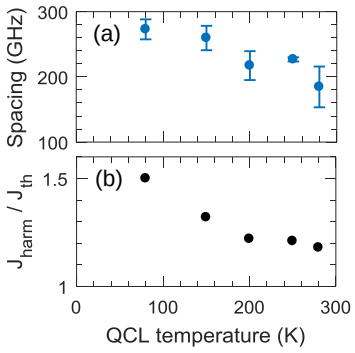

Fig. 8. Influence of the QCL operating temperature on the intermodal spacing of the harmonic state. (a) Measured spacing of the harmonic state as a function of temperature. Error bars correspond to the standard deviation obtained repeating the measurement at each temperature over five consecutive current ramp-ups of the laser. (b) Measured threshold of the single-mode instability corresponding to the appearance of the harmonic state (J_{harm}) normalized to the lasing threshold of the device (J_{th}).

the harmonic state appeared, and the pump current and mode spacing were recorded. By repeating this experiment many times on a single device, we observed different values of the spacing. (Because such variations are not commonly observed on devices outside of a cryostat, we expect that stray reflections from the cryostat windows are responsible for this increased variation.) Each measurement was repeated five times at each temperature, and the results are shown in Fig. 8. The error bars on the harmonic spacing represent the standard deviation across the five measurements. This deviation is significant (up to 17% of the mean value), already indicating that relying on the natural harmonic comb formation in the device is not a convenient method to obtain a fine control of the comb spacing. Despite the statistical uncertainty, we observe two clear trends. First, there is a negative correlation between temperature and harmonic spacing. A possible explanation is the decrease of diffusivity with temperature, which results in stronger population grating contrast and favors smaller sideband separations. However, the variation of upper state lifetime must also be considered in a thorough analysis. Second, there is a positive correlation between the harmonic spacing and the instability threshold. This positive correlation is consistent with the theory: as current increases the detuning of the parametric gain maximum increases, resulting in a predicted increase of the spacing of the harmonic state (cf. Eq. (9)).

3.2. *Optical seeding*

Another possible method for the tuning of the spacing of harmonic combs that we recently explored consists in the injection of an optical seed generated with a broadly tunable external-cavity CW quantum cascade laser (EC-QCL, Daylight Solutions, model 41045-HHG) into the FP-QCL (same device as the one labeled "TL-4.6:HR/AR" in [7]). The seed is focused at an angle of 34° with respect to the normal to the AR facet of the FP-QCL, this angle being larger than the half-divergence angle of the injected laser. This configuration allows for the coupling of a fraction of the optical power of the seed into the cavity of the FP-QCL, while preventing the output of the latter to destabilize the operation of the EC-QCL. The light emitted from the FP-QCL is collimated by an off-axis parabolic mirror, and its emission spectrum is measured using an FTIR. Prior to optical injection the QCL operates in the single mode regime. Injecting an optical seed detuned by 400 GHz with respect to the lasing mode of the free-running QCL destabilizes single mode operation. This effect can be intuitively understood as the result of a competition between the injected seed and the lasing mode for the extraction of gain from the

Optics EXPRESS

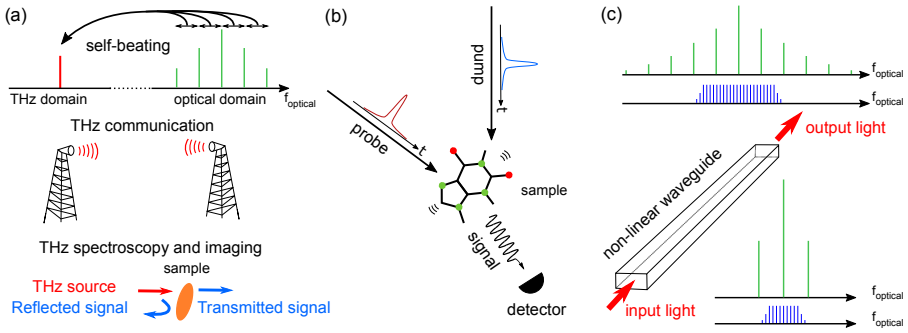

Fig. 9. Prospective applications of the harmonic state of QCLs. (a) The self-beating of the widely-spaced harmonic comb can generate microwave and terahertz radiation which may be used for spectroscopy and wireless communication applications. (b) Short pulses of mid-infrared light used in pump-probe spectroscopy experiments. (c) Broadening the spectral coverage of the harmonic state by means of four-wave mixing in a nonlinear waveguide.

active medium of the laser. By tuning the power of the incident optical seed a variety of laser states can be produced inside the FP cavity, including the harmonic state and an injection-locked single mode. We anticipate here the key result, being that a harmonic state with a well controlled spacing can be triggered by optical seeding. By means of such technique we were able to tune the spacing of the harmonic state in a single device between 0.34 and 1.32 THz.

4. Prospective applications

In the following, we present various prospective applications of the harmonic state of QCLs for which simple illustrations are shown in Fig. 9. First, the self-beating between the modes of the harmonic state can be used to generate microwave and THz radiation (Fig. 9(a)). Second, provided that the harmonic state corresponds to an amplitude modulated temporal waveform, one can use the short pulses emitted by the QCL for pump-probe spectroscopy (Fig. 9(b)). Finally, we propose how to broaden the spectral bandwidth of the harmonic state based on four-wave mixing processes in a non-linear waveguide (Fig. 9(c)).

4.1. Microwave and terahertz generation

The very broad spacing of the highly-correlated modes of the harmonic comb is advantageous for a number of applications, such as the ones requiring access to individual comb lines, e.g. arbitrary optical and microwave waveform generation and others utilizing the coherent beats among the modes to produce stable and spectrally pure tones at the frequency of the comb intermodal spacing. This ability is traditionally exploited by shining the output of a comb source onto a photoconductive antenna or a unitraveling-carrier photodiode that converts intensity oscillations of the optical field into microwave radiation [27, 28]. The very unique feature of QCLs made possible by the ultrashort gain recovery time in these devices is their ability to generate microwave and THz waves directly inside the gain medium, thus dropping the requirement of an external optical-to-electrical converter. This functionality is enabled thanks to the modulation of the vertical current driving the laser induced by the intensity oscillations of the multimode field circulating inside the laser cavity. These modulations exhibit inherently low phase noise, as they arise from the beating of the correlated optical modes. The operation in the harmonic comb regime holds promise for the generation of tones in the microwave (≈1-100 GHz) and THz (0.1-1 THz) spectral regions, and the remarkable tunability of the harmonic comb spacing mentioned in Section 3 should enable to precisely set the desired frequency. From this perspective, the mid-infrared QCL can be seen as a microwave or THz oscillator with adjustable frequency and

Optics EXPRESS

operating at room temperature. Such devices could be suitable for applications ranging from THz imaging and spectroscopy to utilization in quantum optics experiments, where tunable THz sources are needed [29]. Moreover, it was recently proposed that the harmonic comb of QCLs may be utilized for wireless data transfer in the THz range [12]. In such scenarios QCLs are envisioned to operate as compact unibody modems in the THz communication band, as the application of the baseband signal carrying the datastream through the QCL bias line would allow direct intracavity upconversion to the THz carrier that is generated inside the cavity. In this respect the efficiency of the optical-to-microwave/THz conversion and the optimal laser geometry for microwave coupling will need to be explored. This platform may become one of the possible foundations of hardware solutions to the problem of exponentially growing wireless data traffic [28].

4.2. Mid-infrared pulses

In the mid-infrared range short pulses of light can couple to characteristic, fingerprint rotational and vibrational motions of molecules enabling fast molecular spectroscopy [30], which has broad applications in trace gas monitoring, pharmaceutical quality monitoring, and remote detection of biochemical agents, to name a few. To date, the most common approach to generate short pulses in the mid-infrared relies on the down-conversion of short wavelength mode-locked lasers through nonlinear processes such as optical parametric generation or difference frequency generation. These systems are usually bulky, expensive and typically require a complicated optical arrangement. Other types of mid-infrared solid-state lasers that can be mode-locked (active ion-doped crystalline or fiber lasers [31]) operate in a shorter wavelength range around 2-3 μm. Therefore, demonstration of robust and reliable mode locking in QCLs would lead to significant improvement in the state-of-the-art.

Generation of mode-locked pulses in QCLs proved to be challenging. The gain recovery time of a typical QCL is $\approx$1 ps, which is much shorter than the round-trip time of the order of 50 ps in a typical few mm long laser cavity. This effectively prohibits passive mode locking with a saturable absorber of any kind. Indeed, any initial intensity fluctuation in a cavity will get damped if the gain recovers to its small-signal value immediately after the passage of the pulse, leading to preferential amplification of the tails of the pulse. Two approaches to overcome this difficulty have been pursued. In one approach, laser gain is actively modulated to create a window of net gain in a short section of the cavity, which amounts to active mode locking (AML). There has been a widespread belief that a long gain recovery time is essential in this case as well. AML has been observed in THz QCLs where the gain recovery time is believed to be significantly longer than in the mid-infrared QCLs [32, 33]. AML in mid-infrared QCLs was observed in two-section lasers of a design in which the laser transition is diagonal in real space so that the upper-state lifetime can be as long as 40-50 ps [34, 35]. This design compromised laser performance and the mode-locking regime was obtained only close to threshold. However, subsequent theoretical studies [36, 37] indicated that a short gain recovery time in standard high-performance QCLs is not an impediment to AML. This has been experimentally verified for QCLs in an external cavity configuration [38]. The second approach is based on the premise that a phase-coherent frequency comb can be generated by a free-running QCL with a constant-intensity output, provided the QCL is specially designed to have a heterogeneous active region with low GVD. It has been indeed demonstrated that for these low-GVD QCLs, this nearly-constant intensity output can in fact comprise a FM frequency comb, where the phase-locking between the comb teeth is accomplished by the nonlinear four-wave-mixing (FWM) interaction inside the laser cavity [39]. While additional bandstructure engineering will be needed to broaden the bandwidth of these QCL frequency combs, such combs have already proven useful for spectroscopy applications [22]. However, due to the constant intensity of such traditional QCL combs, they will not be useful for any applications that require short pulses of mid-infrared light.

Optics EXPRESS

The harmonic state of QCLs may contradict the conventional wisdom that only FM combs can be generated by free-running QCLs [7]. To understand that in simple terms assume that in the QCL cavity many pulses can circulate per round trip rather than just one, such that the interval between pulses is less than or comparable to the gain recovery time, then the conventional wisdom that the QCL cannot emit a pulse train is incorrect. With more than one pulse circulating per round trip, the QCL does not lase on adjacent FP modes, but rather skips over a number of FP modes equal to the number of pulses per round trip. This is known as harmonic mode locking. For instance, if there are 20 pulses circulating simultaneously in the cavity then the effective roundtrip time is reduced from ≈50 ps by a factor of 20 to 2.5 ps, which is comparable to the gain recovery time. Therefore, in the time interval between two pulses there is not enough time for the gain to fully recover leading to the possibility that a pulse train can perhaps be sustained. This is not to say that the QCL is emitting short pulses every 5.2 ps, instead, there is a slight amplitude modulation that accompanies the appearance of the first sidebands, and the depth of this modulation increases as the number of sidebands increases. In other words, provided that the repetition rate is on the order of the inverse of the gain recovery time or faster, in the harmonic regime the QCL can no longer be considered a fast saturable gain medium, as was previously always assumed [24].

While the possibility of AM operation in a QCL was obtained as a result of the theory of the harmonic state presented in [7], an experimental verification has not yet been reported. In this respect an important point to address in future studies is the measurement of the relative phases of the harmonic modes, which may be achieved by means of a multiheterodyne experiment involving a reference comb with known spectral phase or using spectrum analyzer extension modules in the THz range. Alternatively, second order autocorrelation measurements may shed light on the AM/FM character of the harmonic state, which could exploit the recent advances in sensitive two-photon absorption detectors operating in the mid-infrared range [40, 41].

4.3. Broadband spectroscopy

While the spacing between the modes of the harmonic state is typically much larger than that between the modes of the dense state, the spectral bandwidth of any multimode state of the QCL (harmonic or dense) is limited by its gain spectrum. As a consequence, the harmonic state typically exhibits less than ≈10 comb teeth at the highest pumping currents (see the spectral evolution in Fig. 3). In order to broaden the bandwidth of a harmonic comb, as demanded by spectroscopy applications, one may envision to propagate the light from a QCL through a non-linear Kerr medium, such as silicon. FWM [42] would result in the amplification of the weakest side modes, eventually broadening the initial comb. This scheme could also be used to broaden fundamental QCL combs. However, the net advantage of using a harmonic comb rather than a fundamental comb is that the higher power per mode and broader spacing characteristic of this state are expected to lead to a greater mode proliferation, and thus ultimately to a broader spectral coverage (see Fig. 9(c)).

Previously, nonlinear tapered fibers [43, 44] have been used to generate supercontinuum in the mid-infrared range, while silicon microresonators [45] have been demonstrated for mid-infrared frequency comb generation. While optically-pumped microresonators allow a significant enhancement of the optical nonlinearity, a resonant structure is not ideally suited for the purpose of broadening the spectral coverage of QCL harmonic combs, as the FSR of the two resonators (i.e., the microresonator and the QCL) should precisely match. On the other hand, we expect that silicon waveguides, irrespective of the FSR of the QCL, could be engineered with anomalous dispersion to significantly broaden the spectrum of QCL harmonic combs thanks to the large nonlinearity of silicon. A QCL source could then be integrated along with the nonlinear waveguide resulting in a broadband on-chip frequency comb source.

Optics EXPRESS

5. Conclusions

In summary, we have presented different aspects related to the harmonic state of QCLs, from its natural appearance in the laser to its collapse induced by delayed optical feedback, as well as a thorough experimental characterization of the nature of QCL frequency combs and a theoretical model based on a perturbation theory explaining its formation. Being a recent discovery, several characteristics of this new laser state still remain to be explored. For instance it was observed in certain QCLs that in consecutive current ramp-ups the laser may start on different single mode frequencies triggering harmonic states with different spacing, an interesting phenomenon to be further investigated. A detailed study of the collapse of the harmonic state at high current injection would be also very valuable as it would instruct on possible ways to prevent the transition to the dense state, which is undesirable in practical applications requiring harmonic states at high optical power. In this regard a promising approach would be time-resolved Fourier transform spectroscopy measurements of the spectral evolution of the laser [46]. On the theoretical side, while the present theory of harmonic comb formation [7, 12] provides fundamental insights into the origin of this state, it suffers from the limitations of a perturbation theory. A study of the harmonic regime based on nonlinear space- and time-domain simulations of transport and recombination in the QCL active region is underway and could be used to extract the space and time dependence of any quantity of interest for an operating QCL, such as the intracavity and outgoing EM fields and the electric current across the device, including its beating modulation. To conclude, the ability of skipping modes in a QCL, being the defining feature of the harmonic state, gives a new degree of flexibility in the realm of QCLs, bringing excitement in the field and enabling potential applications previously unforeseen in this platform.

Funding

DARPA SCOUT program (W31P4Q-16-1-0002); National Science Foundation (ECCS-1614631, DGE1144152).

Acknowledgments

Any opinions, findings, conclusions or recommendations expressed in this material are those of the authors and do not necessarily reflect the views of the Assistant Secretary of Defense for Research and Engineering or of the National Science Foundation. N. A. R. is supported by the National Science Foundation Graduate Research Fellowship Program (GRFP) under Grant No. DGE1144152.